Estimating cardiac contraction through high resolution data assimilation of a personalized mechanical model

Henrik Finsberg[a,b,d,1,*], Gabriel Balaban[f], Hans Henrik Odland[c,d], Stian Ross[c,d], Joakim Sundnes[a,b,d], Samuel Wall[a,e,d]

[a] *Simula Research Laboratory, P.O. Box 134 1325 Lysaker, Norway*
[b] *Department of Informatics, University of Oslo, P.O. Box 1080, Blindern 0316 Oslo, Norway*
[c] *Faculty of Medicine, University of Oslo, P.O. Box 1078 Blindern, 0316 Oslo, Norway*
[d] *Center for Cardiological Innovation, Songsvannsveien 9, 0372 Oslo, Norway*
[e] *Department of Mathematical Science and Technology, Norwegian University of Life Sciences, Universitetstunet 3 1430 s, Norway*
[f] *Department of Imaging Sciences and Bioengineering, King's College London, St. Thomas Hospital, Westminster Bridge Rd, Lambeth, London SE1 7EH, UK*

Abstract

Cardiac computational models, individually personalized, can provide clinicians with useful diagnostic information and aid in treatment planning. A major bottleneck in this process can be determining model parameters to fit created models to individual patient data. However, adjoint-based data assimilation techniques can now rapidly estimate high dimensional parameter sets. This method is used on a cohort of heart failure patients, capturing cardiac mechanical information and comparing it with a healthy control group. Excellent fit ($R^2 \geq 0.98$) to systolic strains is obtained, and analysis shows a significant difference in estimated contractility between the two groups.

Keywords:
Cardiac Mechanics, Adjoint Method, Data assimilation, PDE-constrained optimization, Contractility

1. Introduction

Patient-specific cardiac modeling has emerged as a potential tool for clinical diagnosis as well as treatment optimization[**?**]. By linking patient measurements to physical processes through a mathematical framework, models can provide us with additional insight into cardiac function or dysfunction at the level of the individual. However, the complexity of the heart makes this difficult, and this is recognized as a key challenge in modern bioengineering [**?**].

One difficulty is the effort to personalize models and simulations to individual patients. While a wealth of clinical data exists to parameterize such 'patient-specific'

*Corresponding author
Email address: henriknf@simula.no (Henrik Finsberg)

models, methods to assimilate this data into simulations can involve extensive computation time, often putting them outside the scope of clinical utility. However, new methods are emerging to improve the flow of clinical measurements into powerful data driven simulations. Automated geometry segmentation [**?**] and improved optimization techniques [**?**], can improve the speed at which patient-specific models can be built and parameterized. In particular, recent advancements in adjoint-based data assimilation techniques [**?**] offer an efficient way to assimilate ventricular mechanical information using highly spatially resolved parameters.

Here we use an adjoint based assimilation method with a mechanical model in order to construct simulations that accurately reflect clinical motion data, both for healthy controls and patients suffering from left bundle branch block (LBBB). The use of a highly spatially resolved contraction parameter, enabled through adjoint-methods, provides excellent data fit to measured strains and volumes, and fit models provide estimates of cardiac contraction. Such biomarkers may prove useful to clinicians for diagnoses of problems with cardiac function, and to better plan therapies.

2. Materials and methods

2.1. Data acquisition

Clinical measurements of cardiac function for seven LBBB patients were obtained from the Impact study [**?**]. Data was also acquired for seven healthy volunteers. 4D echocardiographic images of the left ventricle (LV), for both the LBBB patients and healthy subjects, were captured using a GE Vingmed E9 device, and analysis carried out with the software package EchoPac. For each subject, depending on frame rate and cardiac cycle time, the analysis provided between 15 and 50 LV volumes, geometric segmentations of the LV endocardium and epicardium, and cardiac strain calculated via speckle tracking. The strains were defined according to the 17 segment AHA-zone representation [**?**], in the longitudinal, radial and circumferential direction, giving a total of 51 strain measurements per time point.

The LBBB patients had LV pressure measurements taken during implantation of a cardiac resynchronization therapy (CRT) device, and valvular events were used to synchronize the pressure to the echo data with the help of a medical doctor. Meanwhile, in the healthy control group, where invasive pressure measurements were absent, the pressure waveform from one of the LBBB patients was used and scaled to reported values of the end-diastolic and end-systolic left ventricular pressure [Table 30-1 in [**?**]].

2.2. Automated geometry and microstructure creation

For each patient, a 3D tetrahedral mesh of the LV was constructed using Gmsh [**?**] from triangulated segmented surfaces of the endo- and epicardium at the beginning of atrial systole, Figure 1. A cut was made at the ventricular base of the segmentation, so that the mesh cavity volume and the ultrasound measured volume differed by less than 1 ml. Mesh cells were marked into the 17 AHA regions through the regionally delineated strain data, and the myocardial fiber orientation were assigned using the algorithm from Bayer et al [**?**], with the endo- and epicardial helix fiber angles set to $\alpha_{\text{endo}} = 60$ and $\alpha_{\text{epi}} = -60$, respectively.

2.3. Mechanical Model

We represent the heart as a hyperelastic continuum body, where the coordinates in the reference($\mathbf{X}$) and the current($\mathbf{x}$) configuration are related via the displacement field $\mathbf{u} = \mathbf{x} - \mathbf{X}$. Furthermore, we utilize the deformation gradient, the determinant of the deformation gradient and, the right Cauchy-Green deformation tensor given by $\mathbf{F} = \mathbf{I} + \nabla\mathbf{u}$, $J = \det\mathbf{F}$ and $\mathbf{C} = \mathbf{F}^T\mathbf{F}$, respectively. To model the passive behavior of the myocardium, the transversely isotropic strain energy function proposed in [**?**] is adopted:

$$\mathcal{W}(I_1, I_{4\mathbf{f}_0}) = \frac{a}{2b}\left(e^{b(I_1-3)} - 1\right) + \frac{a_f}{2b_f}\left(e^{b_f(I_{4\mathbf{f}_0}-1)_+^2} - 1\right). \tag{1}$$

Here $I_1 = \operatorname{tr}\mathbf{C}$ and $I_{4\mathbf{f}_0} = \mathbf{f}_0 \cdot (\mathbf{C}\mathbf{f}_0)$ are invariants of $\mathbf{C}$, $(\cdot)_+ = \max\{\cdot, 0\}$, and a, a_f, b, b_f are material stiffness parameters defining the elastic properties of the myocardium. We follow a common approach and assume that the myocardium is incompressible. Incompressibility is incorporated in the model by using a two-field variational approach, where we introduce a Lagrange multiplier p which represents the hydrostatic pressure, and the term $p(J-1)$ is added to the strain-energy. To model the active response we apply the active strain framework [**?**], decomposing the deformation into elastic and active components, $\mathbf{F} = \mathbf{F}_e\mathbf{F}_a$. The active part, $\mathbf{F}_a$ represents the actual shortening along the muscle fibers, while the elastic part $\mathbf{F}_e$ ensures compatibility of the tissue. We adopt the formulation of the active deformation gradient from [**?**], with the following form:

$$\mathbf{F}_a = (1-\gamma)\mathbf{f}_0 \otimes \mathbf{f}_0 + \frac{1}{\sqrt{1-\gamma}}(\mathbf{I} - \mathbf{f}_0 \otimes \mathbf{f}_0). \tag{2}$$

In this formulation of $\mathbf{F}_a$, γ prescribes the relative active shortening along the fibers, and is implemented as a piecewise linear function over the domain, yielding one parameter per vertex in the mesh. The active model is coupled to the passive model by letting $\mathcal{W}$ in (1) be a function of the modified elastic invariants $I_1^E = \operatorname{tr}\mathbf{C}_e$ and $I_{4\mathbf{f}_0}^E = \mathbf{f}_0 \cdot (\mathbf{C}_e\mathbf{f}_0)$, where $\mathbf{C}_e = \mathbf{F}_e^T\mathbf{F}_e$.

The resulting displacement field $\mathbf{u}$ and hydrostatic pressure p are determined by using the principle of stationary potential energy [**?**], which is based on minimizing the total energy $\Pi(\mathbf{u}, p)$, which includes internal energy derived from (1) and external energy. The external energy includes contributions from the measured cavity pressure p_{LV}, and a linear spring term at the basal boundary, with spring constant $k = 1$ kPa. The equilibrium solution is found by solving for the minimum potential energy, $\delta\Pi(\mathbf{u}, p) = 0$.

2.4. Data Assimilation

In order to constrain the model to each patient's clinical measurements, we consider a PDE-constrained optimization problem where the objective functional is given by the misfit between simulated and measured strain and volume along with a first order Tikhonov regularization of the model parameters.

$$\begin{aligned} \underset{m}{\text{minimize}} \quad & \alpha\left(\frac{V^i - \tilde{V}^i}{V^i}\right)^2 + (1-\alpha)\sum_{j=1}^{17}\sum_{k\in\{c,r,l\}}\left(\varepsilon_{kj}^i - \tilde{\varepsilon}_{kj}^i\right)^2 + \lambda\|\nabla m^i\|^2 \\ \text{subject to} \quad & \delta\Pi(\mathbf{u}, p) = 0. \end{aligned} \tag{3}$$

Here V and ε_{kj} are the measured volume and regional Lagrangian strain in segment j in direction k respectively, and $\tilde{V}^i = -\frac{1}{3}\int_{\partial\Omega_{\text{endo}}}(\mathbf{X}+\mathbf{u})\cdot J\mathbf{F}^{-T}\mathbf{N}\mathrm{d}S$, and $\varepsilon_{kj} = \frac{1}{|\Omega_j|}\int_{\Omega_j}\mathbf{e}_k^T\nabla\mathbf{u}\,\mathbf{e}_k\mathrm{d}x$. The parameters α and λ control the weights on the different terms, and the sum in the second term is taken over the seventeen AHA segments, and the three different strain components (Section 2.1).

The data assimilation procedure is divided into two phases; a passive phase and an active phase. For the passive phase we find the stiffness of the overall ventricle, using the control parameter $m = a$, where a is the linear isotropic parameter in (1), $\alpha = 1.0$, with $\lambda = 0$ and $\gamma = 0$, minimizing only the misfit with the measured volumes. The remaining material parameters are fixed according to [Table 1 row 3 of [**?**]]. For the active phase we fix the material parameter optimized in the passive phase, and the control parameter becomes the pointwise relative mechanical contraction, $m = \gamma$, with $\alpha = 0.95$ and $\lambda = 0.01$. This choice of α and λ was based on the analysis done in [**?**]. A summary of our optimization pipeline is provided to the right in Figure 1.

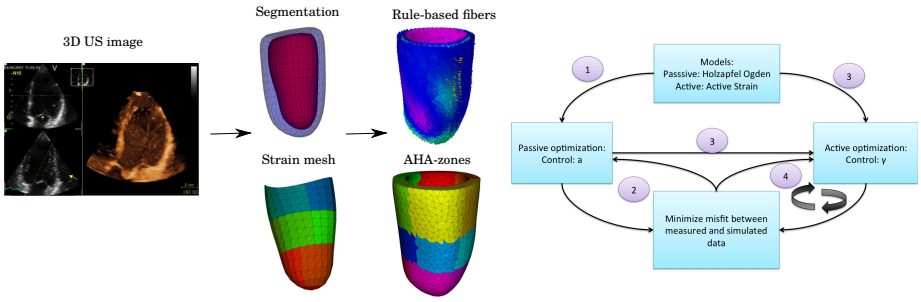

Figure 1: Left: Automated anatomical modeling pipeline to produce AHA marked simulation meshes with applied fiber orientations from 3D echocardiographic segmentations. Right: Optimization pipeline. 1. Optimization of passive model is initialized. 2. Linear isotropic material parameter a in (1) as control parameter, minimize the misfit between simulated and measured volume from beginning of atrial systole to end diastole. 3. Fix the optimized value of a, let γ from (2) be zero, and initialize the active model. 4. Using γ from the previous point as initial guess, minimize the misfit between volume and regional strain using γ as control. Continue until all points in the cardiac cycle are optimized.

2.5. Finite element solution

We employ a Galerkin finite element method with Taylor-Hood tetrahedral elements, that is $(\mathbf{u}, p) \in \mathbb{P}_2 \times \mathbb{P}_1$, with $\mathbb{P}_n$ being the space of piecewise polynomials of degree n. The solver is implemented in the finite element framework FEniCS [**?**], and uses a Newton trust region algorithm [**?**] to solve nonlinear systems. The minimization of the model-data misfit functional (3) is accomplished by a sequential quadratic programming algorithm (SQP) [**?**], where the functional gradient is computed by solving an automatically derived adjoint equation [**?**]. In these minimizations an upper bound of 0.4 is set for the control variable γ.

2.6. Contraction analysis

The optimized spatially resolved contraction parameter γ from (2), may be interpreted as an index of contractility, as it describes how much the material attempts to

contract independent of elastic load. Since this parameter is defined at all the nodal points in the geometry, we summarize the contraction of the LV by averaging over the entire ventricular domain, $\overline{\gamma}(t) = \frac{1}{|\Omega|}\int_\Omega \gamma(t,\mathbf{x})\mathrm{d}\mathbf{x}$, at each time point to provide a trajectory of average ventricular contraction for each patient. In addition, the overall elastic state of the optimized patient models can be used to give estimates of LV elastance. The left ventricular end-systolic elastance E_{ES}, the response of end systolic volume to increased load, is considered to be one of the major determinants for cardiac systolic function, and was in [**?**] proposed as a global index of ventricular contractility. It is possible to calculate the end systolic elastance directly if the end systolic pressure is known or estimated, by perturbing the loading conditions on the optimized model at end systole, and calculating the slope in the resulting ES pressure-volume curve. More precisely, if $p_{\mathrm{lv}}^{\mathrm{ES}}$ is the end-systolic ventricular pressure, with cavity volume V^{ES}, we change the pressure to $p_{\mathrm{lv}}^{\mathrm{ES}+\Delta} = p_{\mathrm{lv}}^{\mathrm{ES}} + \Delta p_{\mathrm{lv}}$, resulting in a change in volume, $V^{\mathrm{ES}+\Delta} = V^{\mathrm{ES}} + \Delta V$. The end-systolic elastance can then be estimated by

$$\tilde{E}_{\mathrm{ES}} = \frac{\Delta p_{\mathrm{lv}}}{\Delta V}. \tag{4}$$

3. Results and discussion

3.1. Matching of strain and volume

We show the results from two representative simulations in Figure 2, one from the LBBB group and one from the healthy control group. Snapshots from the calculated end-diastolic and end-systolic configurations are depicted, and agreement with PV-loops and one of the 51 strain traces over the cardiac cycle shown.

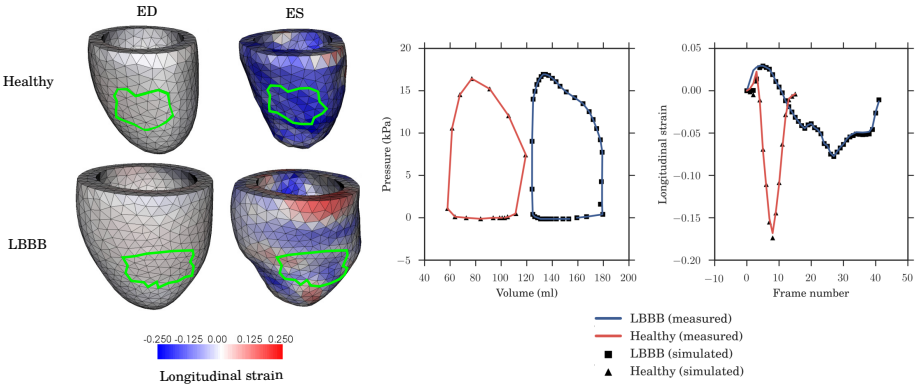

Figure 2: Left: Snap shots of end-diastolic(ED) and end-systolic(ES) model configurations for an LBBB patient and a healthy control. The colormaps shows longitudinal strain. Right: Simulated and measured or estimated pressure-volume loops for these hearts, as well as the longitudinal strain traces for both in the mid septal segment, one of the 51 strain traces optimized. This mid septal segment is highlighted in green in the left figure.

The total analysis of the 14 patients involved optimizing 432 volume measurements and 20 853 strain measurements. The average time for one forward and gradient evalu-

ation was 8.3 and 8.9 seconds respectively when running on a cluster using four cores. Here the average number of control parameters was 985.

In order to visualize the overall match of simulated to measured data, we show linear regression plots in Figure 3. For the strain, we separately consider the diastolic and systolic points, as different types of data were used to constrain the model in these two phases, namely volume in the diastolic phase and strain in the systolic phase. An excellent overall fit was obtained for the optimized volume ($R^2 = 1.00$) and systolic strains ($R^2 = 0.98$). Diastolic strains, not used in the optimization, were less well matched ($R^2 = 0.29$).

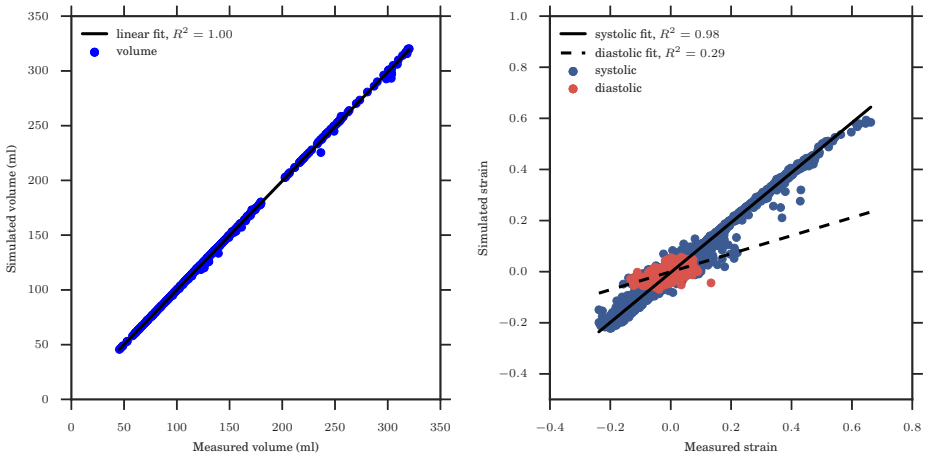

Figure 3: Left: Scatter plot of simulated versus measured volumes and the best linear least-squares fit of these points, (slope = 1.00). Right: Scatter plot of simulated versus measured strain for all segments and all directions, separated into the diastole, were only the volume was optimized and systole, where both the strain and volume were optimized. The best linear least-squares fit for the two cases. For diastole, the slope of the best linear fit was 0.35, while the linear fit for the systolic points had a slope of 0.98.

3.2. Estimation of global contractility and elastance

Global contraction time courses, $\overline{\gamma}$, for each patient were synchronized to the valvular events to normalize for differing cycle lengths. The average and standard deviation of these normalized traces for the LBBB vs the healthy controls are shown in right of Figure 4. The healthy patients had a much higher level of contraction through the cardiac cycle, and the peak values were compared using one-way ANOVA, yielding a $P-$value less than 0.001.

The values of calculated $\tilde{E}_{\mathrm{ES}}$ for the healthy and LBBB patients are shown to the left in Figure 4. The calculated elastances of the LBBB group were significantly lower than for the healthy group, with the comparison between the groups using one-way ANOVA giving a $P-$value of 0.047.

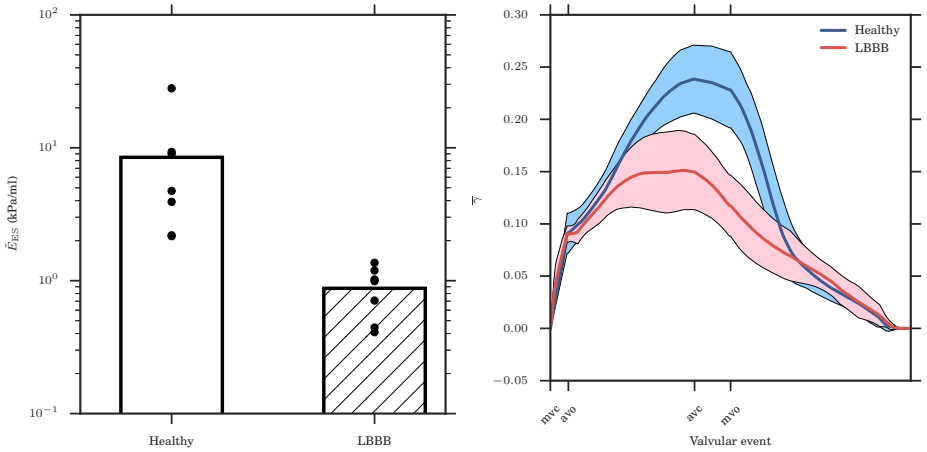

Figure 4: Left: Estimated values of $\tilde{E}_{\mathrm{ES}}$, given by (4). The mean value is depicted for each group as a bar. Right: Mean value of γ for the two groups synchronized with respect to valvular events (mvc: mitrial valve closure, avo: aortic valve opening, avc: aortic valve closure, mvo: mitrial valve opening). Shaded area represents ±1 standard deviation.

4. Discussion

In this study we applied an adjoint-based data assimilation technique to constrain patient data to a cardiac mechanics model. LV pressure was used as a boundary condition, while LV volume and regional strain were assimilated by the means of a spatially varying contraction parameter. We tested this methodology on a group of seven healthy control patients and seven patients diagnosed with LBBB. The results gave an excellent fit between the measured and simulated volume and systolic strain ($R^2 \geq 1.00$ and $R^2 \geq 0.98$, respectively) for more than 21,000 observation points. Diastolic strains, which were not included in the optimization, had a much poorer fit, demonstrating the need for consideration of regional variations in order to create models that can accurately fit patient data.

These calibrated models allow us to quantify aspects of cardiac contractility. We estimated the traditional measure of end-systolic elastance, by perturbations of the model at the end systolic configuration. The healthy control group had significantly higher end-systolic elastance than the LBBB group, although limitations exist with these calculations due to using a synthetic pressure curve with the healthy group. However, the values calculated by using direct pressure readings for the LBBB group (3 - 10 mmHg) are slightly higher but correspond very well with the range provided for a heart failure cohort of (0.5 - 4.9 mm Hg) [**?**]. Along with the end-systolic elastance estimates, our simulations also were use to compare the average value of γ, which may also be interpreted as an index on contractility, between the two groups through the cardiac cycle. Again, the healthy controls showed a significantly higher peak value, compared to the LBBB group. The relationship between γ and $\tilde{E}_{\mathrm{ES}}$ remains to be investigated.

5. Conclusions

Adjoint-based data assimilation are a powerful technique for estimating high dimensional parameters in order to incorporate large amounts of information into a model. Although limitations in our patient data and assumptions remain, we have demonstrated how such techniques can be applied to problems in mechanics for use in estimating indices of cardiac contractility. Future work will be used to adjust and improve such models and work towards their validation and clinical utility.

Acknowledgments

This study was funded by Research Council of Norway: Center for Biomedical Computing at Simula Research Laboratory and Center for Cardiological Innovation at Oslo University Hospital. Computations were performed on the Abel supercomputing cluster at the University of Oslo via a Notur project.